

# HEAT TREATMENT OF DAIRY PRODUCT BY A FLAT OHMIC CELL: IMPACT OF THE REYNOLDS NUMBER, FLUID RHEOLOGY AND FOULING PRESENCE ON THE ELECTRODE SURFACE TEMPERATURE

M.A. Ayadi<sup>a</sup>, T. Benezech<sup>a</sup>, F. Chopard<sup>b</sup>, M. Berthou<sup>c</sup> and J.C. Leuliet<sup>a</sup>

<sup>a</sup> INRA (Institut National de la Recherche Agronomique)

LGPTA (Laboratoire de Génie des Procédés et Technologie Alimentaires)

369, rue Jules Guesde – 59650 VILLENEUVE D'ASCQ cedex – France.

Tel.: (33) 3 20 43 54 40; Fax: (33) 3 20 43 54 26;

Email address: [ayadimedali@yahoo.fr](mailto:ayadimedali@yahoo.fr)

<sup>b</sup> ALFA LAVAL VICARB, rue du Rif Tronchard, 38120 FONTANIL CORNILLON - France.

<sup>c</sup> EDF-R&D, Les Renardières, 77818 MORET SUR LOING Cedex - France.

## ABSTRACT

The aim of this experimental study was to investigate the temperature differences evolution between electrode surfaces and bulk, in a continuous flat ohmic cell under whey protein fouling.

The first part determines the temperature gradients in non-fouled cell using two newtonian fluids (water and an aqueous solution of sucrose at 55% (w/w)) and a pseudoplastic fluid (an aqueous solution of xanthan gum at 0.2% (w/w)). In the second part, the temperature gradients were determined under the same operating conditions except the  $\beta$ -lactoglobulin solutions were used to generate fouling which would be encountered in dairy process. It has been shown that exists a temperature difference between electrode surfaces and the bulk when heating a non-fouling fluids. The value and the shape of these differences depend on the flow regime (Reynolds number) and the rheological behavior of the fluid. Under fouling conditions the temperature differences obtained at different flow regimes exhibit a different trend. Such a difference could be explained by the hydrodynamic behavior of the fluid in addition to the effect of differential electrical conductivities of the bulk and the deposit.

## INTRODUCTION

Dairy products currently represent a large part of food industry productions. The dairy industry keeps developing new milk-based product milk for an increasing consumer demand. Yogurts, creams and milk desserts are some examples of these rheologically complex and highly fouling products. In order to guarantee the health safety and organoleptic quality of the products, industries commonly apply the heat treatments, such as pasteurization and sterilization. Plate heat exchangers are widely used for these treatments. Unfortunately temperature differences between wall and

bulk, due to the hot wall temperature in conventional heating systems, is known to enhance surface fouling (Lalande et al., 1985; René et al. 1991; Belmar-Beiny et al., 1993). Such fouling phenomena is no doubt one of the biggest constraints with this type of apparatus. The overheating of the deposits formed on the hot walls may result in the release of undesirable compounds into the product (cooked taste, lactulose, browning, etc) causing organoleptic alterations. In addition, the development of such deposits may considerably reduce the cross-section and create resistance to heat transfer from the wall to the product, thereby lowering the expected hydraulic and thermal performances of the equipment on the pasteurization or sterilization lines (Delplace et al., 1995; Changani et al., 1997).

Electrical technologies now play a substantial role in this area. Ohmic heating, which appeared at the beginning of the 20<sup>th</sup> century (Anderson and Finkelsten, 1919), continues to develop technologically (Amatore et al., 1998; Roberts et al., 1998; Berthou et al., 2000). The process strong points (simplicity, reliability, no thermal inertia, volume heating) make it, *a priori*, an effective, durable way to resolve the fouling issues. So far most of the research work done with this methodology has focused on tubular devices treating fluids containing particles (Sastry and Salengke, 1998; Marcotte, 1999; Benabderrahman and Pain, 2000; Eliot-Godéreaux et al., 2001). A limited amount of work has been done on heating of homogeneous fouling fluids (Ayadi et al., 2003, 2004a, 2004b).

The objective of this experimental work is therefore to study the evolution of the temperature differences, between the electrode surfaces and the flowing fluid, in a flat ohmic cell when heating non-fouling and fouling fluids.

## MATERIALS AND METHODS

### Fluids used and their physical properties

Xanthan gum (Degussa E415, Texturant Systems; France), sucrose (Semoule la pâtissière, France) and whey protein powder (Protarmor 750; Armor protéines; France) were used to formulate fluids tested in this study.

Two types of fluids with different rheological behaviors were used to carry out the experiments required to study the thermal behavior of an ohmic cell in the absence of fouling phenomena:

Two newtonian fluids were chosen with the aim of observing different flow states, i.e. the transition state with a Reynolds number of 1900 and the laminar state with a Reynolds number of 65 for a flow rate of 300 L/h. Fluids used were water and sucrose solution at 55% (w/w).

A pseudoplastic fluid was used in addition to the above newtonian fluids to determine the temperature profiles in the non-fouled ohmic cell. This fluid was an aqueous solution of xanthan gum 0.2% (w/w).

Two fouling model fluids were formulated to study temperature gradient evolution in fouled ohmic cell: (i) an aqueous solution of native whey proteins (1 wt% of protein powder) and (ii) an aqueous mixed solution of native whey protein (1 wt%) and xanthan gum (0.2 wt%). The choice of these model fluids was based on the fact that the heat denaturation of  $\beta$ -lactoglobulin protein governs milk deposit formation when the temperature exceeds 75°C (Lalande *et al.*, 1985).

The model fluids were prepared with great care to ensure that their physical properties remained constant for all the tests. To prevent any change to the physical property, model fluids were prepared and stored at 4°C for 12 h before the fouling experiments. Their density, specific heat and thermal conductivity are very close to those of water. The protein-xanthan mixture fluid exhibits shear-thinning behaviour characterised by consistency  $k$  and flow index  $n$  given by

$$n = 0.0023 \theta + 0.234$$

(1)

$$k = 6.78 \theta^{-0.663} \quad (2)$$

where  $\theta$  is the temperature in degree Centigrade and  $k$  is in Pa.s<sup>n</sup>. These parameters were obtained from regression of data collected over a temperature range of 20-80°C and shear rates from 0.4 to 700 s<sup>-1</sup>.

With the temperature range from 10 to 100°C, the evolution of the electrical conductivity of each fluid was modeled by the following equations:

$$\text{For the aqueous solution of } \beta\text{-lactoglobulin :} \\ \sigma(\theta) = 0.0318 \cdot \theta + 0.7449 \quad (3)$$

For the aqueous solution of  $\beta$ -lactoglobulin-xanthan mixture :

$$\sigma(\theta) = 0.0363 \cdot \theta + 0.6762 \quad (4)$$

### Geometry and instrumentation of the ohmic heater

The ohmic heater was made up of an arrangement of five ohmic cells, three of them ensuring heating and the two side cells ensuring electric insulation and the recovery of leakage currents. Each cell can be compared to a rectangular channel (length = 0.240 m; width = 0.75 m and thickness = 0.015 m), the electrodes constituting side surfaces.

In the case of ohmic heating, the presence of an electrical field makes measurement of the fluid temperature a delicate matter since the sensor may dissipate energy dissipation by the Joule effect, thereby masking the measurement results. In addition, the sensor should have minimal flow disturbance since local temperature rise depends on the residence time in the cell and the presence of a recirculation zone or dead zone, even a reduced one, due to the presence of the sensor may lead to erroneous measurements.

Taking into account these constraints, the last heating cell (cell n°4) of the ohmic module was instrumented with 27 type J Iron-Constantan thermocouples (diameter 0.001 m). As shown in Figure 1, 24 thermocouples were implanted on the walls of the cell (12 thermocouples per electrode) so as to obtain a temperature measurement representative of a 15x10<sup>-4</sup> m<sup>2</sup> surface area.

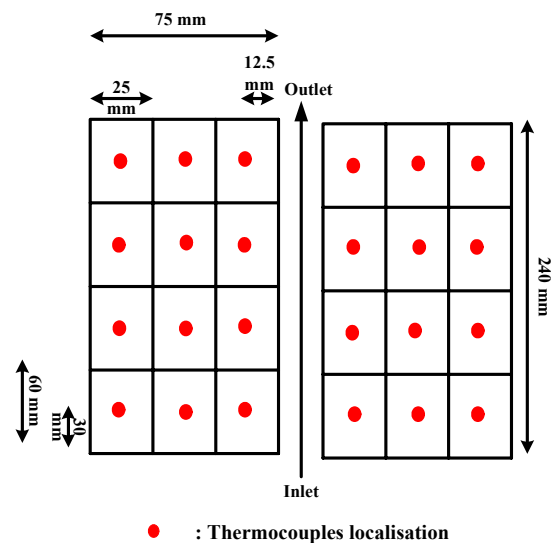


Fig. 1: Position of thermocouples on the electrode surfaces of the last heating cell (cell n°4).

The last three thermocouples, were coated with a very thin Teflon film (total diameter of thermocouple + sleeve is 0.0012 m) to prevent any Joule effects. Two of the three thermocouples were inserted in the inlet and outlet of the cell and the end of the third thermocouple

was bent so that the fluid temperature measurement could be taken before the flow was disturbed by the measurement tool. This thermocouple also allows temperature measurements to be taken at any point in the studied section by means of intrusion and movement systems installed at the cell spacer ( $z = 0.21$  m) as shown in Figure 2. The accuracy of temperature measurements was  $\pm 0.3^\circ\text{C}$  for all the thermocouples.

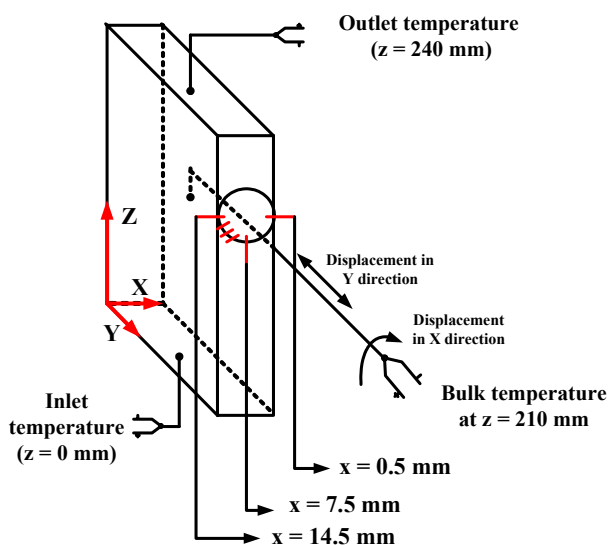


Fig. 2: Bulk temperature measurement in the last heating cell (cell n° 4) of the ohmic module.

Representation of the system used to insert and move the thermocouple in a measurement section.

### Fouling trials

The pilot-plant test rig used in the fouling trials is shown in Figure 3.

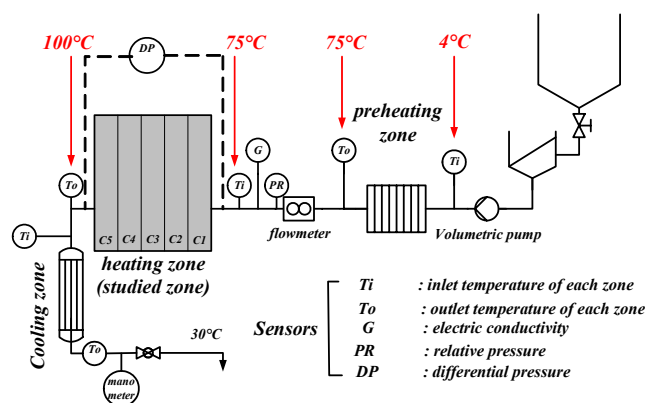


Fig. 3: Pilot-plant test rig.

It consists of three parts: (i) a preheating zone with a plate heat exchanger, (ii) a heating zone with an

arrangement of five flat ohmic cells, and (iii) a cooling zone with a tubular heat exchanger. In addition, a storage tank ( $2\text{ m}^3$ ), a constant level tank and a volumetric feed pump were necessary to perform the tests. A manual throttling valve at the outlet allowed us to control the backpressure.

The flowrate was measured using an electromagnetic flowmeter (Khrone, type: IFM 10807K). Temperatures were measured by means of platinum resistance probes (Sensor-Nite, type: Pt 100) placed at the inlet and outlet of each zone. A differential pressure sensor (Schlumberger, type: D) was used to follow the pressure drop increase in ohmic cells. The electric power supply was determined using voltage measurements between the second and third electrodes (Voltmeter 0-250V, Sineax U504, Chauvin Arnoux) and the intensity of the second phase of the electric transformer (Ammeter 0-200A, type AC22, Camille Bauer).

All signals were treated (module SCX-1) and collected using a data acquisition card (AT-MOI-16E-10). A software driver (Ni-DAQ) provided the configuration and control of data acquisition system. Data were stored using Labview software systems.

## RESULTS AND DISCUSSION

### Temperature profiles in non-fouled ohmic cell

Figure 4 shows the temperature profiles along the thickness ( $0 < x < 15\text{ mm}$ ) and the width ( $0 < y < 75\text{ mm}$ ) of the cell, for three different fluids (water, 55% (w/w) sucrose solution and a 0.2% (w/w) aqueous xanthan solution). To allow the comparison between these results, the temperatures were normalized according to the temperature at the cell's inlet.

Figure 4 firstly indicates that whatever the axis (X or Y), whatever the fluid and whatever the regime (laminar or turbulent), the fluid near to the wall is always warmer (to varying degrees) than at the centre of the channel.

In the case of water, this temperature gradient did not exceed  $2^\circ\text{C}$ . Consequently, the temperature profile appears flat along the complete measurement section. This result was to be expected, as the flow regime encountered with this fluid is the transitory regime (close to a turbulent regime). This result confirms the previous results obtained by Muller et al. (1993) and (1994) with ohmic heating technology in tubular geometry and those obtained by Ould El Moktar et al. (1993) when heating water in a flat ohmic cell.

The 55% (w/w) sucrose solution is a Newtonian fluid, which is sufficiently viscous to enable the observation of a laminar flow (its viscosity being 15 times that of water). This fluid has the particularity of its

viscosity being strongly temperature dependent. The temperature gradient between the wall and the center of the channel is almost 9 times that of water. This observation may only be explained by the modification in the general appearance of the velocity profile and consequently in residence time distribution. In effect, the velocity profiles are flattened in the centre of the flow, in a turbulent flow regime (as in the case of water) and forms a parabolic profile in a laminar flow regime. In the case of the sucrose solution, the velocity is therefore far higher at the center of the channel than at the walls. Fluid particles circulating in the parietal zone are thus submitted to the effects of the electric field for longer periods and are heated to a greater extent than those at the center of the channel. On the other hand, by drawing up temperature profiles along the thickness axis ( $x$ ) in Figure 4b, it was observed that the temperature profile at  $y = 0\text{mm}$  is significantly different from the others, the fluid was clearly warmer. These results highlight the fact that, unlike conditions under turbulent flow regime, in a laminar regime the slowdown in the flow rate in the right angled corners of the rectangular section induced an increase in the fluid temperature, which was significant throughout the entire passage section.

The 0.2% aqueous xanthan solution whose viscosity was close to 15 times that of water for the operating conditions determined for this study (shear rate and temperatures) presented a pseudoplastic rheological behavior. Observing of the results presented in Figure 4c, it is possible to see that all the  $y$ -axis temperature profiles were similar to those obtained with the sucrose solution. It should be pointed out, however, that the temperature did not significantly rise from the point where  $y = 15\text{mm}$ , thereby indicated a constant temperature throughout the section between 15 and 37 mm. This difference was explained by the lower thermo-dependence of xanthan solution comparing to that of the sucrose solution. At the wall, the apparent viscosity was lower due to high shear rate conditions. Only  $10^\circ\text{C}$  in the temperature increase was observed compared to  $25^\circ\text{C}$  observed with the sucrose. A deformation in the temperature profiles for  $y = 0$  and  $y = 7\text{mm}$  is visible, whatever the thickness. This is translated both by higher temperatures than those recorded for the other planes ( $y = 14, 21, 28$  and  $35\text{mm}$ ) and also by a significant heating of the fluid in the vicinity of the walls. The shape of these temperature profile ( $y = 0$  and  $y = 7\text{ mm}$ ) could be explained by the buoyancy forces generated by the probable huge differences in the apparent viscosity of this shear-thinning

fluid. In quite the same way as for the sucrose solution, we are able to underline the impact of the right angles during the treatment of pseudoplastic fluids by a rectangular ohmic cell.

As fouling phenomena are closely linked to temperature heterogeneity this thermal behaviour may have considerable consequences during the treatment of fouling fluids.

### Temperature profiles in fouled ohmic cell

Figure 5a, show the evolution of the temperature gradient between the electrode surfaces and the bulk recorded during a 4-h fouling run. It is interesting to note that this figure presents an increase in the parietal temperature during the first three hours. The latter reaches maximal values and then falls rapidly until it becomes very close to the temperature displayed by the thermocouple in the bulk. This evolution may be explained by the fouling of the thermocouple placed in the bulk. Effectively, it is clear that fouling phenomena are closely linked to flow and to the temperature in the vicinity of the walls. Consequently, at the outset, the electrodes' surfaces become fouled much faster than that of the thermocouple placed in the bulk. The Joule effect of these deposit layers lead to an increase in the temperature of the electrodes. This would, in effect, explain why at the beginning of the run, it was observed a significant difference between the temperatures displayed by the two thermocouples. As the run progressed, the deposit layer which adhered on the thermocouple in the bulk builds up considerably and therefore also become the seat of an electrical energy dissipation due to the Joule effect, inducing an increase in the temperature of the deposit around the thermocouple placed in the bulk. This result thus explained the decrease in the measured temperature gradient so that it practically reached zero (measurement of the Joule effect in the both two deposits). In order to illustrate this clearly, Figure 5b presents the photo of the two thermocouples and the electrode just after the fouling run.

Given these results, we can state that it is very difficult to observe the evolution in the temperature gradient between the wall and the bulk by measuring the temperature of the fluid with a thermocouple submitted to the effects of an electrical field. This leads us to assess the temperature in the bulk theoretically, supposing a linear temperature profile between the inlets and outlets of the three heating cells and the isothermal conditions of the lateral non-heating cells.

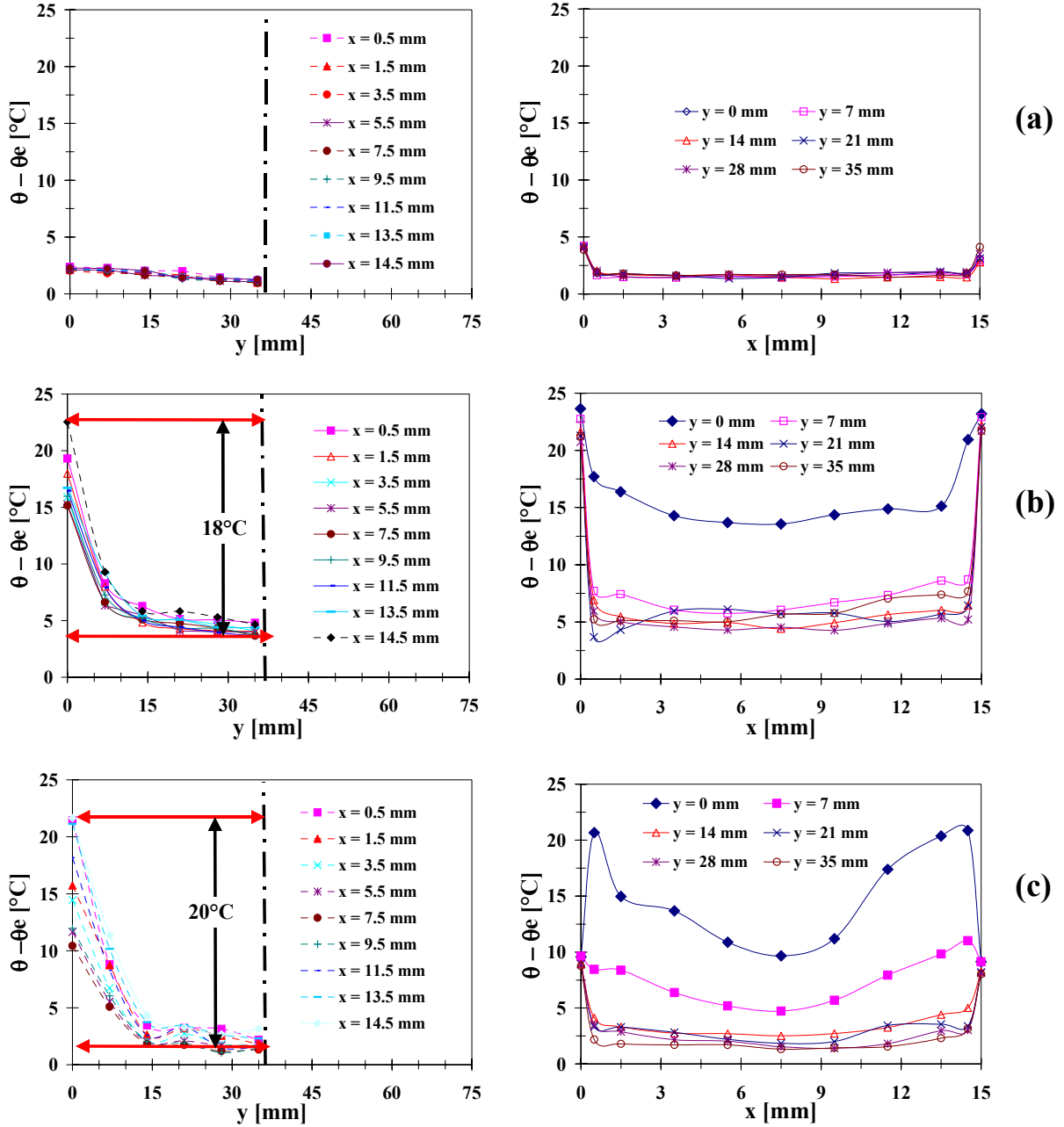


Fig. 4: Temperature profiles recorded at the outlet ( $z = 210\text{mm}$ ) of the ohmic cell at various points in the width ( $y$ ) and the thickness ( $x$ ): (a) water; (b) 55% (w/w) aqueous sucrose solution and (c) 0.2% aqueous xanthan solution.

Taking these hypotheses into account, the temperature gradients between the wall and the bulk in the third heating cell (cell n°4) are estimated in the following manner:

Isothermal Conditions :

$$\theta_{E.C1} = \theta_{E.pdt} = 75^\circ\text{C} \text{ and } \theta_{S.C4} = \theta_{S.pdt} = 100^\circ\text{C}$$

Linear Profile: For  $z = 0$ ,

$$\theta_{E.C4} = \theta_{E.pdt} + \frac{2}{3} \cdot (\theta_{S.pdt} - \theta_{E.pdt}) \quad (5)$$

For  $0 \leq z \leq L$ ,

$$\theta_{z.C4} = \theta_{E.C4} + \frac{z}{L} \cdot (\theta_{S.pdt} - \theta_{E.pdt}) \quad (6)$$

The difference in temperature between the fluid and the electrode surface  $\Delta\theta(x, z)$ , at the coordinates  $(x, z)$  may thus be written :

$$\Delta\theta(x, z) = \theta_{Th}(x, z) - \theta_{z.C4}(x, z) \quad (7)$$

with  $\theta_{Th}(x, z)$  the surface temperature measured at coordinates  $(x, z)$ .

The nondimensional temperature gradient ( $T^*(x, z)$ ) is calculated in the following manner:

$$T^*(x, z) = \frac{\Delta\theta(x, z)}{\theta_{S.C4} - \theta_{E.C4}} \quad (8)$$

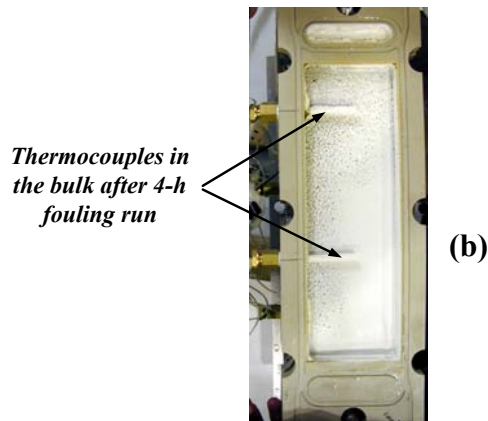
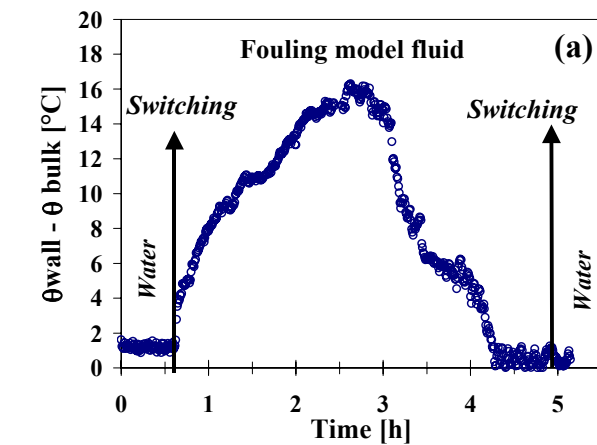


Fig. 5: Measurement of the temperature in the bulk during a 4-h fouling run: (a) evolution in the difference between the wall temperature and the bulk one; (b) photo of the thermocouples in the bulk.

Figure 6 shows the evolution of the temperature gradient during 4-h fouling experiments. First of all, this figure shows that the gradient between the wall and the bulk does not exceed 2°C before switching from water to the fouling solution thereby confirming the previously

obtained results. Then an instantaneous overheating occurs when heating the fouling fluid formulated with xanthan gum ( $Re = 65$ ). This overheating may be explained by the change in viscosity (change from water to fouling fluid) and consequently the shape of the velocity profile. hence, it confirmed results obtained during the study of the thermic performances of a non-fouled ohmic cell. In effect, the model fouling fluid was at the same viscosity as the 0.2% aqueous xanthan solution previously used. The change-over from water to model fouling fluid caused an increase in the temperature gradient of around 8°C ( $T^* = 1$ ). After the change-over to model fouling fluid, the local temperature gradient curves present two different evolutions depend on the flow regime.

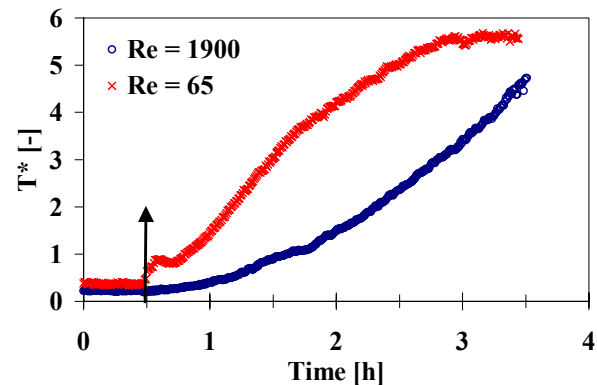


Fig. 6: Reduce local temperature gradient evolution during 4-h fouling runs (the temperature in the bulk was estimated, using equation 5, that of the wall was experimentally measured): ( $z = 210\text{mm}$ ).

For the laminar flow, no significant increase in the temperature gradient was visible for a shorter period (the first few minutes of the run). Then a significant increase in the temperature gradient was observed, which reached a high level (6 times the heating value in the cell  $\approx 48^\circ\text{C}$ ). Finally, at the end of the run the curve takes on an asymptotic shape and local temperature gradient disturbances were observed. As for the laminar flow, in the case of the turbulent flow a very slight increase in the temperature gradient was visible for a shorter period (the first few minutes of the run). Then an exponential evolution was observed. These curves shapes could be explained as following : during the first minutes, the deposit was not enough significant to detect a joule effect in it. So that we did not observe any increase in the temperature gradient. When the deposit became significant it acted as an electrical resistance and the deposit received more and more electrical energy so that its temperature continuously increased. It would be interesting to evaluate the energy dissipation both in the

fluid and the deposit. Figure 7 shows an equivalent electric circuit of a fouled ohmic cell.

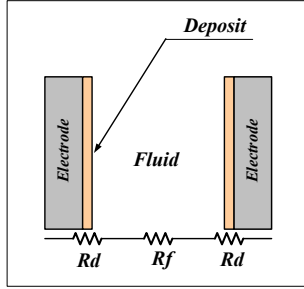


Fig. 7 : Equivalent electric circuit of fouled flat ohmic cell

In the above figure, the resistance of the electrodes is negligible compared to the other components. Then, if a voltage  $V$  is applied across the system, we have the following relations.

$$I = \frac{V}{R_d + R_f + R_d} \quad (9)$$

and the voltage drop through the deposit sections is:

$$V_d = IR_d = \frac{VR_d}{2R_d + R_f} \quad (10)$$

and the voltage drop through the fluid section is:

$$V_f = IR_f = \frac{VR_f}{2R_d + R_f} \quad (11)$$

Since the current is equal in all cases, the energy generation ( $=VI$ ) within each section (deposit or fluid) depends only on the applied voltage. Thus:

$$Q_d = V_d I = \frac{VR_d I}{2R_d + R_f} \quad (12)$$

and

$$Q_f = V_f I = \frac{VR_f I}{2R_d + R_f} \quad (13)$$

Thus:

$$\frac{Q_d}{Q_f} = \frac{R_d}{R_f} \quad (14)$$

$$\text{Since: } R_d = \frac{e_d}{A\sigma_d} \text{ and } R_f = \frac{e_f}{A\sigma_f}$$

so

$$\frac{Q_d}{Q_f} = \frac{l_d \sigma_f}{l_f \sigma_d} \quad (15)$$

It is clear that the energy dissipated in both fluid and deposit depend on their relative thickness and electrical conductivities. Typically the thickness of the deposit is considerably smaller than that of the fluid (i.e.  $l_f \ll l_d$ ). In addition, Ayadi et al., (2004c) showed that the electrical conductivity of the deposit is lower than that of the heated fluid and the electric conductivity of the deposit generated by ohmic heating of an aqueous solution of  $\beta$ -lactoglobulin-xanthan mixture is higher than electric conductivity of deposit generated by heating a aqueous solution of  $\beta$ -lactoglobulin. Both effect of higher electrical conductivity and better heat exchange at the wall under turbulent flow regime could explain the observed shape of the temperature gradient at  $Re = 1900$ .

## CONCLUSIONS

The study of thermal behavior of a flat ohmic cell when heating fouling and non-fouling fluid, shows that as with conventional heat exchangers, a temperature differences exists between wall and bulk. In non-fouling conditions this temperature gradient depend on the flow regime and the fluid rheological behavior. Under fouling condition as soon as deposition on the electrode surfaces takes place, it acts as an additional electrical resistance subject to the Joule effect. The dissipation of the electrical energy into the deposit layers causes an increase in its temperatures. It would appear that the evolution in the temperature gradient depends on both the deposit electrical conductivity and the flow regime. Based on this experimental study, a significant step will be done by redesigning the electrodes so as to avoid any passage of electrical current in hydrodynamically disturbed zones, as the edges of straight angles.

## NOMENCLATURE

Q	dissipated electric power, W
Y	cell length, mm
Z	cell height, mm
X	cell thick, mm
x	x-axis coordinate, mm
y	y-axis coordinate, mm
z	z-axis coordinate, mm
Re	Reynolds number
$\theta$	bulk temperature, °C
$\theta(y,z)$	bulk temperature in the fourth cell at y,z coordinate, °C
$\theta_{Th}(x,z)$	surface temperature measured at x,z coordinate
$\Delta\theta(y,z)$	temperature variation between bulk and electrodes surfaces at y,z coordinate, °C
$T^*(y,z)$	reduced temperature variation between bulk and electrodes surfaces at y,z coordinate.
n	flow behavior index.

e thickness; mm  
 $\sigma$  electrical conductivity, mS cm<sup>-1</sup>

### Subscript

f fluid  
d deposit  
E inlet  
S outlet  
C<sub>1,2,3,4 and 5</sub> cells number

### REFERENCES

Amatore, C., Berthou, M., Hébert, S., 1998, Fundamental Principles of Electrochemical Ohmic heating of Solutions, *Electroanalytical Chemistry*, vol. 457, pp 191-203.

Anderson, A.K., Finkelsten, R., 1919, A Study of the Electro-pure Process of Treating Milk, *Journal of Dairy Science*, Vol.2, pp. 374 – 406.

Ayadi M.A., Bouvier L., Chopard F., Berthou M. and Leuliet J.C. (2003). Heat treatment improvement of dairy products via ohmic heating process: thermal and hydrodynamic effect on fouling. in the proceedings of the Engineering Conference International (ECI) : Heat Exchanger Fouling and Cleaning-Fundamentals and Applications (eds P. Watkinson, H. Muller-Steinhagen and M. R. Malayeri)

Ayadi M.A., Leuliet J-C., Chopard F., Berthou M. and Lebouché M, (2004)c, Electrical conductivity of whey protein deposit: xanthan gum effect on temperature dependency, *TransIcheme Part C: Food and Bioproducts processing*, 82 (4), pp 320-325.

Ayadi M.A., Leuliet J-C., Chopard F., Berthou M. and Lebouché M., (2004)a, Ohmic heating unit performance under whey proteins Fouling, *Innovative Food Science & Emerging Technologies*, 5 (4), pp 465-473.

Ayadi M.A., Leuliet J-C., Chopard F., Berthou M. and Lebouché M., (2004)b, Experimental study of hydrodynamic behaviour in a ohmic cell: impact on fouling by whey proteines, *Journal of Food Engineering*, (in press).

Belmar-Beiny, M.T., Gotham, S.M., Paterson, W.R., and Fryer, P.J., 1993, The Effect of Reynolds Number and Fluid Temperature in Whey Protein Fouling, *Journal of Food Engineering*, vol. 19, pp. 119-139.

Benabderrahmane, Y., Pain, J.P., 2000, Thermal Behaviour of a Solid/Liquid Mixture in an Ohmic Heating Sterilizer – Slip Phase Model, *Chemical Engineering Science*, Vol. 55, pp. 1371-1384.

Berthou, M., Aussudre, C., 2000, Panorama sur le Chauffage Ohmique Dans l'Industrie Agro-alimentaire, *Industries Alimentaires & Agricoles*, n°7/8, pp. 31-38.

Changani, S.D., Belmar-Beiny, M.T. and Fryer, P.J., 1997, Engineering and Chemical Factors Associated with

Fouling and Cleaning in Milk Processing, *Experimental Thermal and Fluid Science*, Vol. 14, pp 392-406.

Delplace, F., Leuliet, J.C., 1995, Modeling Fouling of a Plate Heat Exchanger with Different Flow Arrangements by Whey Protein Solutions, *Trans Ichem*, Vol.73, pp. 112-120.

Eliot-Godéreaux, S., Zuber, F., Goullieux, A., 2001, Processing and Stabilisation of Cauliflower by Ohmic Heating Technology, *Innovative Food Science & Emerging Technologies*, Vol. 2, pp. 279-287.

Lalande, M., Tissier, J.P., Corrieu, G., 1985, Fouling of Heat Transfer Surfaces Related to  $\beta$ -lactoglobulin Denaturation During Heat Processing of Milk, *Biotechnology progress*, Vol.1, pp. 131-139.

Marcotte, M., 1999, Ohmic Heating of Viscous Liquid Food, Ph.D. thesis, Department of Food Science and Agricultural Chemistry, University Mc Gill, Canada.

Muller, F.L., Pain, J.P., Villon, P., (1993), Chauffage ohmique des liquides non-Newtoniens, 6<sup>ème</sup> colloque TIFAN, Tome VI, 229-236.

Muller, F.L., Pain, J.P., Villon, P., (1994), On the behaviour of Non-Newtonian Liquids in Collinear ohmic heaters, in proceedings of the Tenth International Heat Transfer Conference, Brighton, UK, 4, 285-290.

Ould El Moktar, A., Peerhossaini, H., Bardon, J.P., (1993), Effet de la convection naturelle lors du chauffage de fluides complexes par conduction électrique directe, 6<sup>ème</sup> colloque TIFAN, Tome VI, 217-228.

Peng, X.F., Huang, Y.J., Lee, D.J., 2001, Transport Phenomenon of a Vapour Bubble Attached to a Downward Surface, *Int. J. Therm. Sci*, Vol. 40, pp 797-803.

René, F., Leuliet, J.C., Lalande, M., 1991, Heat Transfer to Newtonian and non-Newtonian Food Fluids in Plate Heat Exchangers: Experimental and Numerical Approaches, *Trans IChemE*, Vol. 69, Part C, pp. 115-126.

Roberts, J.S., Balaban, M.O., Luzuriaga, R.Z.D., 1998, Design and Testing of a Prototype Ohmic Thawing Unit, *Computers and Electronics in Agriculture*, Vol. 19, pp. 211-222.

Sastry, S.K., and Salengke, S., 1998, Ohmic Heating of Solid-Liquid Mixtures: A Comparison of Mathematical Models Under worst-case Heating Conditions, *Journal of Food Process Engineering*, Vol. 21, pp 441-458.

### ACKNOWLEDGEMENT:

The authors gratefully acknowledge the financial support from Alfa Laval Vicarb and Electricité de France.